OAK RIDGE NATIONAL LABORATORY

operated by

UNION CARBIDE CORPORATION

for the

U.S. ATOMIC ENERGY COMMISSION

ORNL-TM-121

UNIT OPERATIONS SECTION MONTHLY PROGRESS REPORT

OCTOBER 1961

NOTICE

This document contains information of a preliminary nature and was prepared primarily for internal use at the Oak Ridge National Laboratory. It is subject to revision or correction and therefore does not represent a final report. The information is not to be abstracted, reprinted or otherwise given public dissemination without the approval of the ORNL patent branch, Legal and Information Control Department.

LEGAL NOTICE

This report was prepared as an account of Government sponsored work. Neither the United States, nor the Commission, nor any person acting on behalf of the Commission:

A. Makes any warranty or representation, expressed or implied, with respect to the accuracy, completeness, or usefulness of the information contained in this report, or that the use of any information, apparatus, method, or process disclosed in this report may not infringe privately owned rights; or

B. Assumes any liabilities with respect to the use of, or for damages resulting from the use of any information, apparatus, method, or process disclosed in this report.

As used in the above, "person acting on behalf of the Commission" includes any employee or contractor of the Commission, or employee of such contractor, to the extent that such employee or contractor of the Commission, or employee of such contractor prepares, disseminates, or provides access to, any information pursuant to his employment or contract with the Commission, or his employment with such contractor.

ORNL-TM-121

UNIT OPERATIONS SECTION MONTHLY PROGRESS REPORT

October 1961

CHEMICAL TECHNOLOGY DIVISION

M. E. Whatley

P. A. Haas
R. W. Horton
A. D. Ryon
J. C. Suddath
C. D. Watson

Date Issued

APR - 5 1962

OAK RIDGE NATIONAL LABORATORY
Oak Ridge, Tennessee
Operated By
UNION CARBIDE CORPORATION
for the
U. S. Atomic Energy Commission

ABSTRACT

Additional runs were made in the 6-in.-dia separation column. The kinetics of the methane-copper oxide reaction was investigated in deep bed tests. The work on the development of the shear included a satisfactory method of holding a fuel assembly during shearing, preliminary tests of an outer gag faced with rubber and a metallic inner gag contoured to the shape of a sheared assembly. The mechanical dejacketing of the SRE Core I fuel, NaK bonded, stainless steel clad uranium slugs, was successfully completed. The effective thermal conductivity of a packed bed of 0.023 in. steel shot was approximately 0.33 BTU/hr-°F-ft at 200°F. Flow capacity for the compound extraction scrub column equipped with sieve plates (0.125-in.-dia holes, 23% free area) for the amine extraction flowsheet was determined. Average waste calcination rates for Purex were higher by a factor of 1.5 to 2.0 than rates for TBP-25.

CONTENTS

		Page
	Abstract	2
	Previous Reports in this Series for the Year 1961	4
	Summary	5
1.0	Chemical Engineering Research	8
2.0	GCR Coolant Purification Studies	13
3.0	Power Reactor Fuel Processing	18
4.0	Reactor Evaluation Studies	27
5.0	Solvent Extraction Studies	33
6.0	Waste Processing	37

Previous Reports in this Series for the Year 1961

January	ORNL CF 61-1-27
February	ORNL CF 61-2-65
March	ORNL CF 61-3-67
April	ORNL-TM-32
May	ORNL-TM-33
June	ORNL-TM-34
July	ORNL-TM-35
August	ORNL-TM-65
September	ORNL-TM-112

All previous reports in this series are listed in the June 1961 report, ORNL-TM-34, from the beginning, December 1954.

SUMMARY

1.0 CHEMICAL ENGINEERING RESEARCH

Foam Separation

Additional runs were made in a 6-in.-dia foam separation column with the 10^{-3} M NaOH, 10^{-4} to 10^{-3} M dodecylbenzenesulfonate and 10^{-3} to 10^{-6} M $Sr(OH)_2$ system. The surfactant distributions were 7.2×10^{-4} (moles/cm^2)/(mole cm^3). The values calculated for Sr distributions from the experimental data were 3 to 4 x 10^{-3} (moles/cm^2)/(mole/cm^3) for Sr concentrations below 10^{-5} M/ However, precipitation of $SrCO_3$ from absorption of CO_2 from the foam generating gas or the air above the feed liquid probably occurred during the initial four experimental runs. The continuous countercurrent runs were made with liquid/surface flow ratios much smaller than the optimum and did not give useful column efficiency data.

2.0 GCR COOLANT PURIFICATION STUDIES

The kinetics of the methane-copper oxide reaction was investigated in deep bed tests. In the range investigated (10 to 30 atm and 400 to 600°C), the rate was dependent on methane concentration and CuO surface area.

3.0 POWER REACTOR FUEL PROCESSING

3.1 Shear and Leach

The economic and technological feasibility of shearing and leaching spent power reactor fuels is to be determined initially in a "cold" chop and leach facility consisting of a shear, conveyor feeder, and leacher.

In continuing development of a satisfactory method of holding a fuel assembly during shearing, preliminary tests of an outer gag faced with rubber and a metallic inner gag contoured to the shape of a sheared assembly were very encouraging.

The stepped moving blade of the shear has made about 800 cuts on a stainless steel jacketed porcelain filled Mark I prototype with no signs of wear.

Preliminary design of the shear-leach complex auxiliary equipment is essentially complete.

Design of the electrical control circuit for manual and automatic operation of the conveyor-feeder and leacher has been completed.

3.2 SRE Dejacketing Studies

The mechanical dejacketing of the SRE Core I fuel, NaK bonded, stainless steel clad uranium slugs, was successfully completed. A total of 1,780 kg of uranium slugs, 0.75-in.-OD x 6-in. long were dejacketed,

steam cleaned, recanned in aluminum, and stored to await off-site shipment for processing. The overall average processing rate, based on actual operating time, was ~6 kg U/hr.

The decay heat from a can of 12 slugs in storage in air was measured at 2.5°F above the ambient storage room temperature of 87°F.

An oil fire produced from a NaK-water reaction was quickly extinguished with CO_2. Damage to equipment was minor and only about 1 hr of operating time was lost.

3.3 U-C Fuel Processing

An acceptable uranium loss was not attained in any of the semicontinuous leach runs in which -4 mesh graphite fuel (2.6% U) was leached in 90% HNO_3 at 60°C. The leaching cycle consisted of a 2 hr batch leach followed by a 4 hr leach in flowing acid, and a final water wash. Uranium losses to the residue were 1.5%, 1.6%, 0.61%, and 0.56% at flow rates of 0.52, 0.91, 1.52, and 2.21 bed volume changes per hour, respectively.

4.0 REACTOR EVALUATION STUDIES

Heat Transfer from Spent Reactor Fuels during Shipping

The effective thermal conductivity of a packed bed of 0.023 in. steel shot was measured to assess the possibility of using such a material to aid in removing heat from spent reactor fuels in shipping casks. The measured value was a slightly increasing function of temperature and had a value of approximately 0.33 Btu/hr-°F-ft at 200°F.

5.0 SOLVENT EXTRACTION STUDIES

Work was started to evaluate the flow capacity and stage efficiency of pulse columns as a function of operating variables and cartridge design for the amine extraction flowsheet for final cycle plutonium recovery. Flow capacity for the compound extraction scrub column equipped with sieve plates (0.125-in.-dia holes, 23% free area) and operated aqueous continuous was > 2400 gal $ft^{-2}hr^{-1}$ at 50 cpm pulse frequency and was 1590 gal $ft^{-2}hr^{-1}$ at 30 cpm for a similar column equipped with nozzle plates (0.125-in.-dia nozzle, 10% free area) and operated organic continuous. Flow capacity for sieve plate stripping column (aqueous continuous operation) was 540 gal ft^{-2} hr^{-1} at 35 cpm and for the nozzle plate column (organic continuous operation) was 440 gal $ft^{-2}hr^{-1}$ at 35 cpm.

Flow capacity in the sieve plate solvent treatment column operated aqueous continuous at phase ratio (A/O) of 1/2 was 375 gal $ft^{-2}hr^{-1}$ and < 100 gal $ft^{-2}hr^{-1}$ at a phase ratio of 1/3.3. Flow capacity of the sieve plate column operated solvent continuous at phase ratio of 1/3.3 was > 700 gal $ft^{-2}hr^{-1}$. The nozzle plate solvent treatment column operated with the solvent phase continuous at 1/3.3 phase ratio flooded at 350 gal $ft^{-2}hr^{-1}$.

6.0 WASTE PROCESSING

Preliminary results from continuous flowsheet conditions for Purex and TBP-25 type waste indicate average rates for Purex to be higher by a factor of 1.5 to 2.0 than rates for TBP-25. Prolonged feed periods for TBP-25 type waste gave higher bulk densities (0.77 g/cm^3) at the expense of decreased average feed rates. A revision of the continuous evaporator was necessary to give sufficient boil-up for peak Purex conditions.

1.0 CHEMICAL ENGINEERING RESEARCH

1.1 Foam Separation - P. A. Haas, J. D. Sheppard

Engineering studies of countercurrent foam-liquid columns were continued with the objective of evaluating the engineering variables which control column performance. Additional runs were made with the NaOH-dodecylbenzenesulfonate-Sr^{++} system selected as a simple chemical system to simplify the analyses of results. This system was found to be more complex than assumed (August Unit Operations Monthly Progress Report) and a more complicated analyses of results will be necessary.

Isotopic Exchange Equilibrium. The system selected for investigations of column efficiency was isotopic exchange of Sr using radioactive Sr-89. The equilibrium distribution of the strontium forms of the surfactant will not show any detectable variation due to the strontium isotope. At equilibrium, the ratios of Sr-89/Sr_T where Sr_T is the total strontium will be the same in the bulk liquid and at the surface. The Sr-89 concentration is easily measured by use of its radioactivity.

Experimental results have shown that the surface/solution separation factors for various cationic complexes of a surfactant are nearly independent of cation.* A simple method of measuring concentrations of the dodecylbenzenesulfonate surfactant was available.** If all the surfactant were present as cationic complexes and all the Sr was complexed, the ratios of Sr_T/DBS where DBS indicates the dodecylbenzenesulfonate surfactant would be identical in the bulk liquid and at the surface. The sodium salt of dodecylbenzenesulfonate is over 90% ionized at 10^{-4} M concentrations and the ionic form is relatively non-surface active. Therefore, Sr_T/DBS is much larger at the surface than in the bulk solution.

Values of $\Gamma/C = 1.7 \times 10^{-2}$ cm or 1.7×10^{-2} (moles Sr/cm^2)/(moles Sr/cm^3) have been reported for conditions usable for column efficiency tests.*** This value can be used to calculate Sr_T concentrations, but the accuracy is poor because of the poor accuracy of foam surface area measurements. The foam column system will be arranged to permit checking of Sr_T concentrations at the countercurrent run conditions by use of the Sr-89 tracer without isotopic exchange. Future countercurrent runs will be made using flow ratios calculated to be optimum for the correct equilibrium curve and checked by the single stage Sr_T concentration measurement mentioned above.

Effects of CO_2 Absorption. The presence of $CO_3^{=}$ in the solution from absorption of CO_2 from the atmosphere or the foam generating gas results in precipitation of relatively insoluble $SrCO_3$. The conditions which would result in precipitation can be estimated from:

---

* ORNL CF 61-2-61, "Monthly Progress Report for Chemical Development Section B, January 1961, p. 35-39.

** ORNL-TM-65, "Unit Operations Monthly Progress Report, August 1961."

*** E. Schonfeld, ORNL, personal communication, October 1961.

a. The solubility product of $SrCO_3$ at 25°C is 1.6×10^{-9} (moles/liter)^2.

b. The CO_2 content of fresh air will average 0.04% or 400 ppm by volume.

c. The CO_2 content of H_2O pumped N_2 at Oak Ridge has been found to be 30 to 40 ppm.

d. The solubility of CO_2 is water at 25°C is 0.76 scc/cc H_2O for a CO_2 pressure of 760 or 0.145 g/100 g H_2O for a CO_2 pressure of 735 mm.

e. The equilibrium CO_2 concentration in the gas for absorption in NaOH solutions is very small for $CO_3^{=}/Na^+ < 0.5$ and becomes significant for $CO_3^{=}/Na^+$ between 0.5 and 1.0.

f. Feed gas rates were 3000 cc/min.

g. The liquid feeds were 0.001 M NaOH and were 2×10^{-6} to 5×10^{-4} M Sr. The amounts of Sr were 54 to 3000 μ moles for batch tests and 0.6 to 61 μ moles/min for continuous countercurrent tests.

From the gas rates and concentrations, precipitation of $SrCO_3$ was probable for most of the continuous countercurrent runs and was possible for all of them if some pickup of CO_2 by the feed prior to entry into the column was assumed (Table 1.1). Precipitation of $SrCO_3$ should not have resulted during batch runs 10, 11, and 12, but may have occurred during runs 7 and 9. Since solids are surface active, any $SrCO_3$ precipitate would pass through the column with the foam and result in Sr in the condensed foam which would be incorrectly attributed to the effect of the surfactant.

Countercurrent Run Results. The principal useful results from three countercurrent runs has been the refinement of operating procedures. The material balances for surfactant using the ultraviolet absortivity as a method of analysis** were 84 to 101% with most of them 90 to 101%. Adequate sampling procedures and adequate containment of tracer in other respects was demonstrated.

No useful data on column efficiencies was obtained. The precipitation of $SrCO_3$ probably contributed to the transfer of Sr from the liquid to the surface for all runs. All liquid/surface flow ratios were selected much smaller than optimum because of the incorrectly assumed equilibrium curve.

Batch Test Results. Five batch tests were made in order to investigate unexpected countercurrent continuous results. These tests involved putting a batch charge of feed containing Sr-89 in the column and collecting condensed foam samples without any continuous liquid feed or countercurrent contact. The surface surfactant concentrations from runs 7 and 9 (Figure 1.1) are about 150% of those reported from laboratory measurements. Areas of

Table 1.1. Effects of CO_2 in Foam Generating Gas

Run No.	Total Liquid Input	Sr Input	CO_2 Input	Estimated % Sr ppt as $Sr\ CO_3$[a]
A. Continuous countercurrent runs:				
	cc/min	μ moles/min	μ moles/min	
5A	150	0.7	48	0
5B	100	0.6	48	45
5C	300	1.4	48	0
6A	150	1.32	48	43
6B	110	1.0	48	59
6C	125	1.12	48	53
6D	210	1.88	48	22
8A	110	29.4	48	97
8B	135	41.6	48	93
8C	125	36.7	48	95
8D	160	53.9	48	81
8E	175	61.2	48	74
B. Batch runs:				
	cc	μ moles	μ moles	
7	6000	54	3840	72
9	6000	< 5	6720	0
10	6000	2940	~0	0
11	7000	350	~0	0
12	7000	1750	~0	0

[a] Based on CO_2 free solution at start of run, solubility constant = 1600 (μ moles/liter)^2.

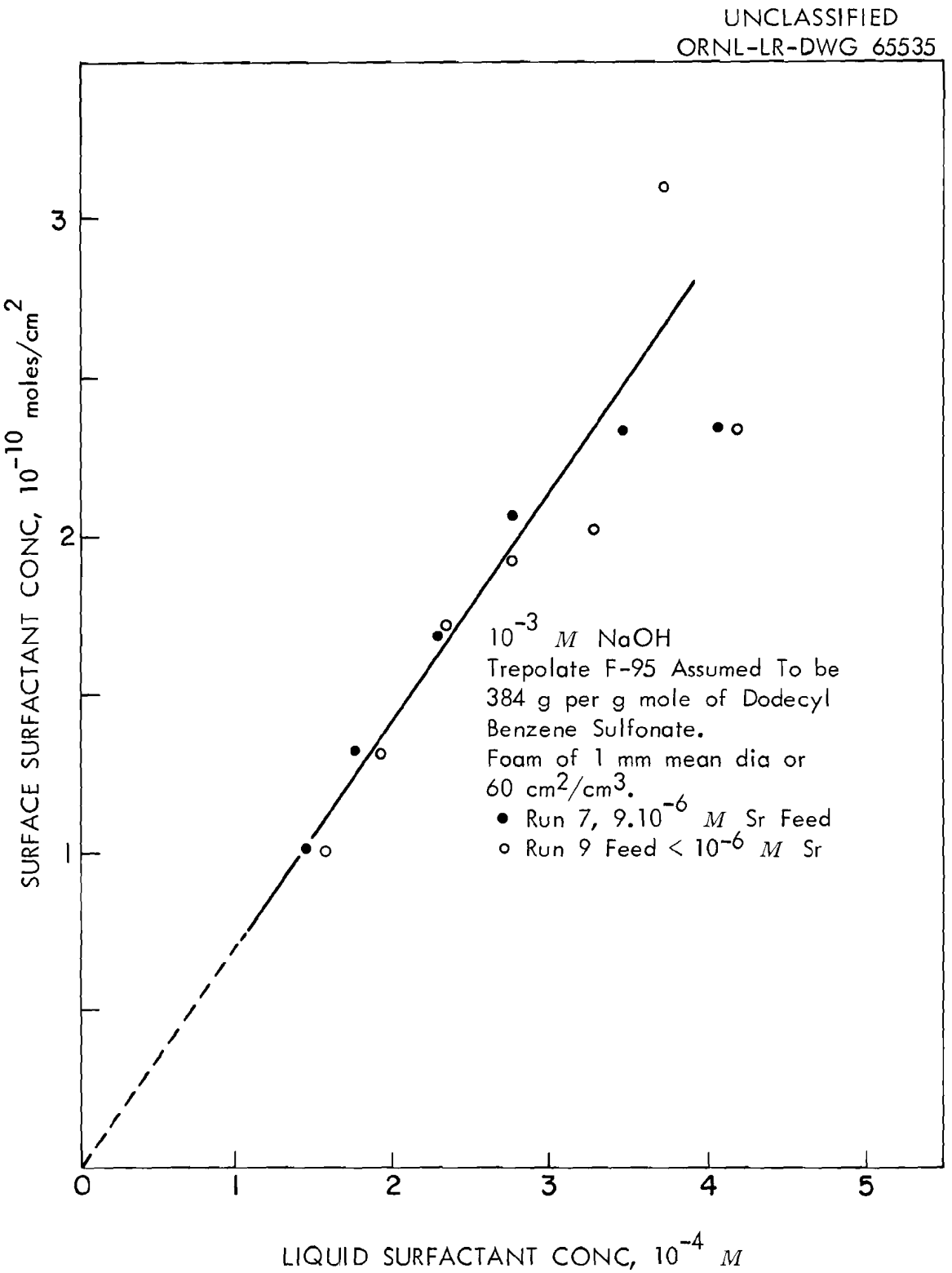

Fig. 1.1. Surface liquid surfactant distribution.

90 cm^2/cm^3 of foam might be more correct than 60 cm^2/cm^3 for the foam leaving the liquid. Use of 90 cm^2/cm^3 would result in verification of the laboratory values. The slope of Figure 1.1 corresponds to Γ/C = 7.2×10^{-4} cm or 7.2×10^{-4} (moles/cm^2)/(mole/cm^3). The validity of values of Γ/C for Sr are uncertain due to the possibility of $SrCO_3$ precipitation. The calculated values are about 3×10^{-3} cm for run 7 and 4×10^{-3} cm for run 9. Results from runs 10, 11, and 12 are not complete.

2.0 GCR COOLANT PURIFICATION STUDIES

J. C. Suddath

Contamination of coolant gases by chemical impurities and release of fission products from fuel elements are major problems in gas-cooled reactors and in-pile experimental loops. Investigations are being made to determine the best methods to reduce the impurities, both radioactive and non-radioactive with emphasis on the kinetic mechanisms of the fixed bed oxidation of hydrogen, carbon monoxide and methane by copper oxide.

The reaction rate of the CH_4-CuO reaction appears to be dependent on CH_4 concentration and available CuO surface area. Several deep bed tests seem to confirm this dependence.

2.1 Kinetics of the CH_4-CuO Reaction - C. D. Scott

A total of six kinetic tests were made on the reaction of CH_4 from a flowing stream of helium with fixed beds of CuO pellets. The ranges of operating conditions were:

System pressure - 10.2-30.0 atm
System temperature - 400-600°C
Mass flow rate - 0.086-0.169 g-moles/cm^2-min
Gas phase methane concentration - 0.31-0.53 vol %
CuO bed volume in 2-in.-dia reactor - 49-196 cc

The deep bed system can be represented by the following differential equations if the reaction is dependent on methane concentration and CuO surface area:

Bed Material Balance:

$$\left(\frac{\partial C}{\partial t}\right)_z + V\left(\frac{\partial C}{\partial z}\right)_t = \frac{1}{4\beta}\left(\frac{\partial n}{\partial t}\right)_z \qquad (1)$$

Reaction Rate:

$$\left(\frac{\partial n}{\partial t}\right)_z = - k\,K\,Cn^{2/3} \qquad (2)$$

where,

C = gas-phase methane concentration, g-moles/cc

t = reaction time, sec

z = bed height measured from bottom of bed, cm

V = interstatial gas velocity, cm/sec

β = bed external porosity, void volume/total volume

n = molar density of CuO in CuO bed, g-moles/cc

k = reaction rate constant which is dependent on temperature

K = constant dependent on physical properties of the CuO pellets

Equations (1) and (2) can be used to predict the gas-phase methane concentration at any point in the CuO fixed-bed and they may be solved simultaneously by finite difference methods which are amenable to digital computer techniques.

These equations were solved on the IBM 7090 computer at ORGDP Computing Center for the conditions of each of the six deep bed tests made. The effluent methane concentration as a function of time was computed for each test. These predicted effluent methane concentration history curves were then compared to the actual experimental data from the six deep bed tests (Figures 2.1 - 2.3). It was found that there was an acceptable fit of the predicted values with the experimental data over the range of experimental data. The experimental data scatter was much greater for the CH_4-CuO reaction than for the reaction of H_2 or CO with CuO. This probably reflects the larger temperature dependence of the CH_4-CuO reaction and the temperature fluctuation during the experimental tests ($\pm$ 25°).

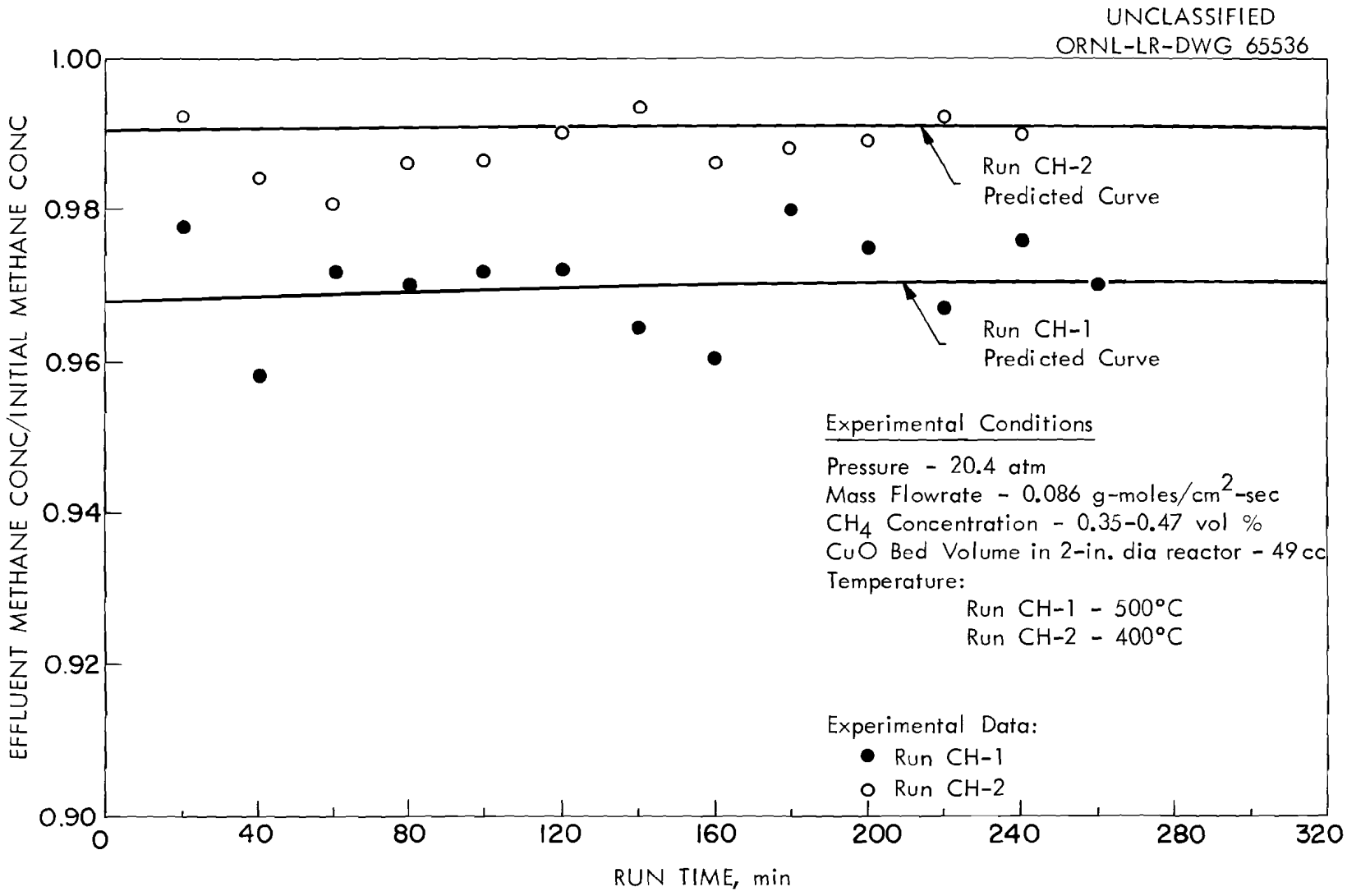

Fig. 2.1. Comparison between experimental data and predicted effluent concentration history curves for the CH_4-CuO reaction showing the influence of reaction temperature.

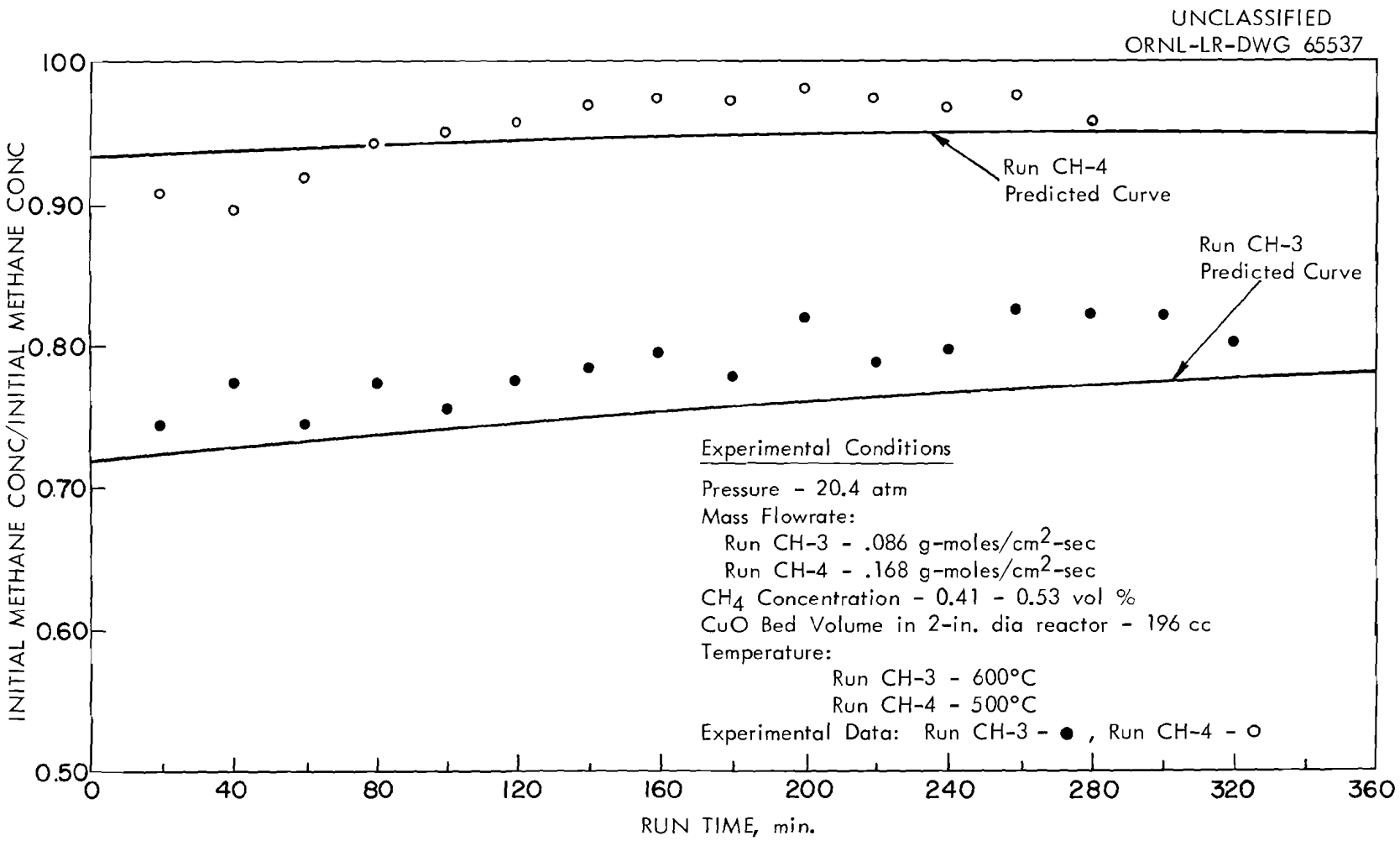

Fig. 2.2. Comparison between experimental data and predicted effluent concentration history curves for the CH_4-CuO reaction showing the influence of mass flowrate.

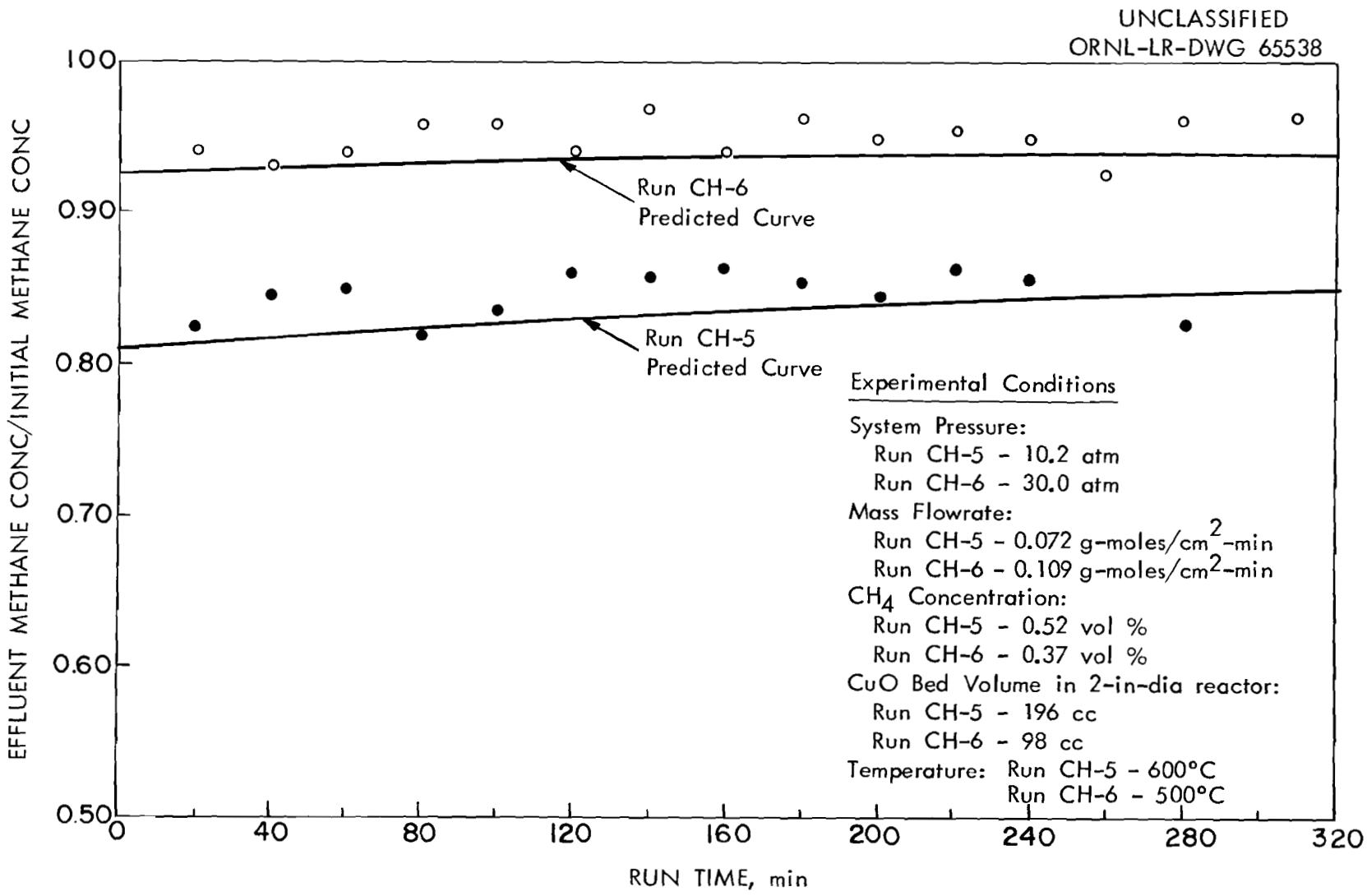

Fig. 2.3. Comparison between experimental data and predicted effluent concentration history curves for the CH_4-CuO reaction at the two pressures, 10.2 atm and 30.0 atm.

3.0 POWER REACTOR FUEL PROCESSING

C. D. Watson

3.1 Shear and Leach - B. C. Finney

A shear and leach program to determine the economic and technological feasibility of continuously leaching the core material (UO_2 or UO_2-ThO_2) from relatively short sections (1-in. long) of fuel elements produced by shearing is continuing. This processing method enjoys the apparent advantage of recovering fissile and fertile material from spent power reactor fuel elements without dissolution of the inert jacketing material and end adaptors. These unfueled portions are stored directly in a minimum volume as a solid waste. A "cold" shear-leach complex consisting of a shear, conveyor feeder, and leacher is being evaluated prior to "hot" runs.

The development of a satisfactory method of holding or gagging a tubular prototype fuel assembly during shearing is continuing. Gagging is a three-fold problem, (1) the fuel assembly must be held securely during shear, (2) the fuel assembly must be progressively fed into the shear against the stop after each cut, and (3) the fuel assembly should be sheared to within 1 inch of the end. Tests to date have been made shearing across the diagonal of porcelain filled ORNL Mark I fuel assemblies with a double row of ferrules every 12 inches using a stepped blade with a rubber insert in the outer gag and metal insert in the inner gag. The blade tends to crush and deform the end of the assembly which assumes an approximate 30 degree slope at the cut end. The slope increases to approximately 45 degrees when the sheared face is at or through a double row of ferrules (Figure 3.1). This changing face of the bundle prevents proper feeding by jamming against the contoured face of the inner gag. Jamming can be eliminated by deliberately retracting the inner gag at the appropriate time so that the deformed cut end of the bundle does not come in contact with the gag. However, retracting the gags even partially has resulted in end pieces of from 1-1/2 to 2 inches long falling into the shear. Attempts to move the fuel assembly forward by retracting the outer gag and leaving the inner gag in position but reducing the pressure to zero has been unsuccessful. Two fresh approaches to the gagging problem have developed, (1) spring load the inner gag so that it will retract easily when contacted by the fuel assembly and thus conform it to the changing shape of the fuel assembly, (2) shear into the flat side of a fuel assembly rather than on the diagonal to minimize deformation of the sheared face thus permitting easier feeding by the gags.

The Squarkeen No. 3 (American Knife Co. alloy equivalent to Carpenter 610) stepped moving blade of the shear hardened to a Rockwell C of ~59 has made about 800 cuts on stainless steel jacketed porcelain filled ORNL Mark I prototype fuel assemblies with no sign of wear (Figure 3.2).

Preliminary design of the shear-leach complex acid feed, product handling, and off-gas handling equipment is essentially complete.

UNCLASSIFIED
PHOTO 56093

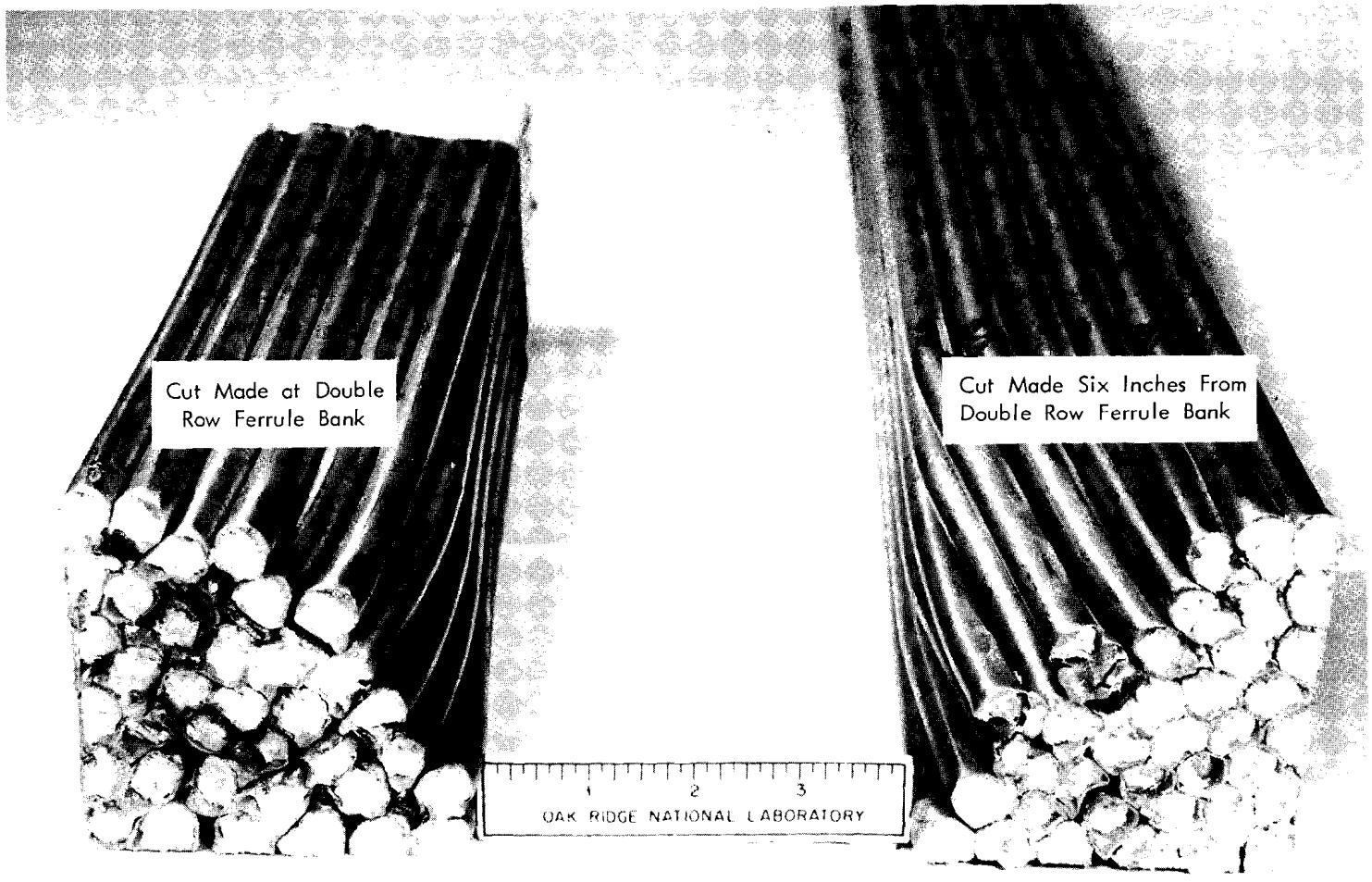

Fig. 3.1. Comparison of bundle shape using a stepped movable blade to shear across the diagonal of a porcelain filled ORNL Mark I fuel assembly.

UNCLASSIFIED
PHOTO 56096

Fig. 3.2. Squarkeen No. 3 movable stepped blade after making approximately 800 cuts on stainless steel jacketed porcelain filled ORNL Mark I prototype fuel assemblies.

Installation of the conveyor-feeder and leacher control circuitry is approximately 75% complete.

3.2 SRE Dejacketing Studies - G. A. West

Mechanical dejacketing of the SRE Core I fuel, NaK bonded, stainless steel jacketed uranium slugs, 2.77% enriched, burned to ~675 MWD/ton and decayed ~2 years, was successfully completed in the ORNL High Level Segmenting Facility, Bldg. 3026-D.

A total of 26 canisters of fuel rods containing 1,778 kg of uranium slugs, 0.75-in.-OD x 6-in.-long, were dejacketed, steam cleaned, recanned, and placed in storage to await off-site shipping and processing. The surface temperature of cans of slugs stored in a critically safe array was measured 2.5°F greater than the 87°F storage room temperature. Terminal processing rates of from 2.3 kg/hr to 7.7 kg/hr were attained. The low rate resulted from the processing of a canister containing embrittled and broken rods (Figure 3.3) which required ~30 hrs processing time. The 8 ft long rods required cutting of the jacket near each slug juncture and removal of the jacket by splitting with the auxiliary dejacketer cutters or with a special chisel.

Ten jacketed slugs in a basket stored in the steam cleaner for 64 hrs were reduced to a sludge of uranium oxide (Figure 3.4) by leaking steam and condensate. The 10 mil thick jackets were split by expansion of the uranium slugs as it was converted to the oxide. The 8.2 kg of uranium oxide sludge in the steam cleaner basket and steam cleaner filter was placed in double containment cans and buried underground.

Sections of stainless steel jackets ~4 in. long from the center rods of the clusters were removed for physical property analysis.

NaK samples were obtained from the center rods of all clusters. Results from five different clusters show the following activities, no uranium or plutonium were found:

	1	2	3	4	5
Cs^{137} (c/m/g)	9.9×10^5	2.6×10^6	9.0×10^5	1.6×10^6	2.1×10^6
Gross γ (c/m/g)	9.24×10^6	2.66×10^7	8.92×10^6	1.71×10^7	2.11×10^7
Gross β (c/m/g)	4.25×10^6	1.13×10^6	4.32×10^6	7.25×10^6	9.59×10^6
TRE β (c/m/g)	2.36×10^3	8.59×10^4	3.72×10^3	2.33×10^3	2.39×10^3
Gross α (c/m/g)	nil	nil	nil	nil	nil
U (mg/ml)	< 0.0001	< 0.0001	< 0.0001	< 0.0001	< 0.0001
Na (%)	24	21	24	24	25
K (%)	76	79	76	76	75
O_2 (ppm)	2708	6785	5905	2473	2963

In general the operation of the mechanical equipment complex for the dejacketing of SRE Core I fuel was satisfactory. However, due to the extreme hardness and embrittlement of the irradiated stainless steel jackets, the physical force required to perform each step was much greater than

UNCLASSIFIED
PHOTO 55633

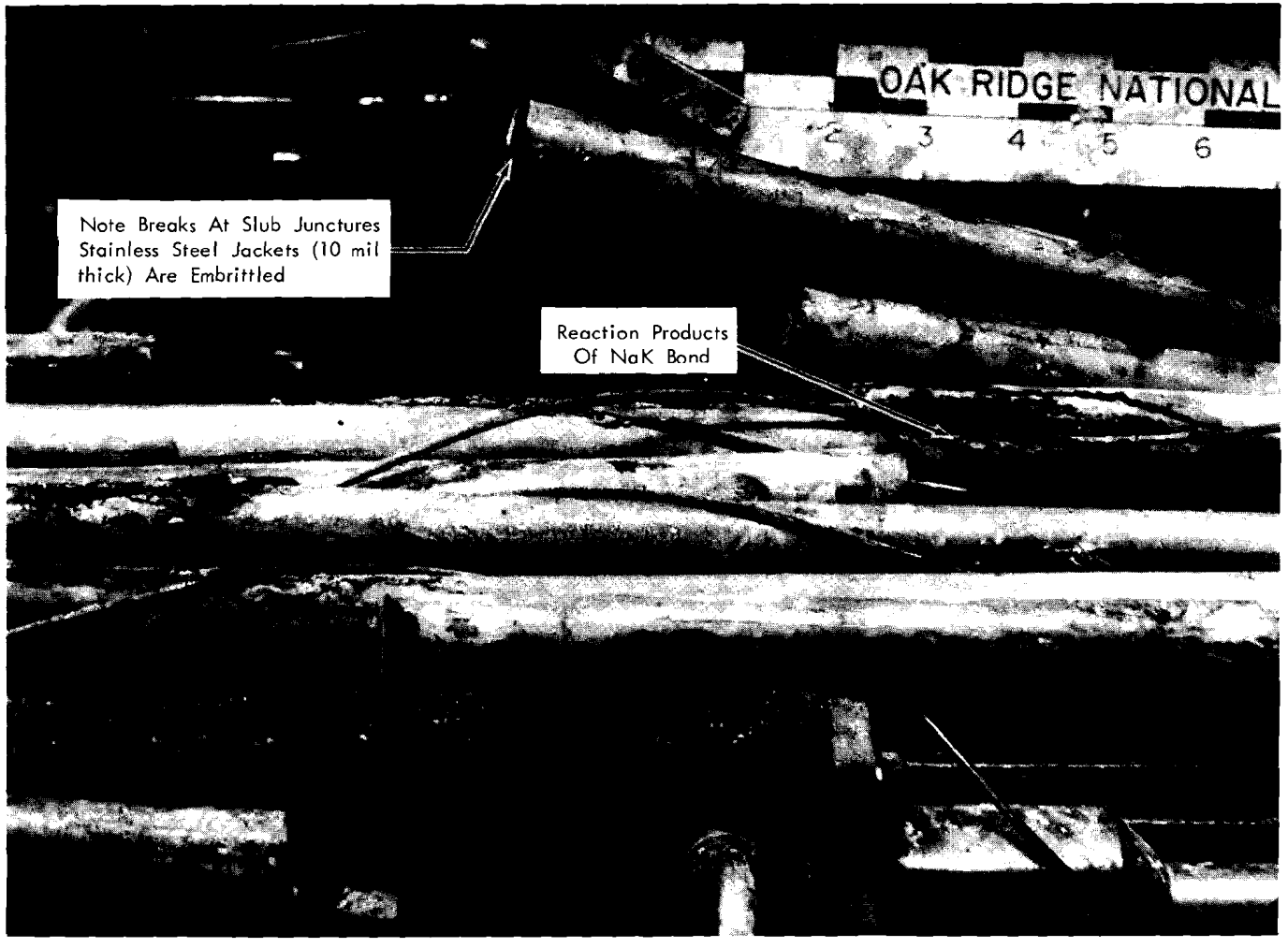

Fig. 3.3. Condition of 7 rod SRE core 1 fuel cluster as withdrawn from shipping canister (~ 675 Mwd/ton, cooled ~ 2 yr) (photographed through 5 ft. thick zinc bromide window).

UNCLASSIFIED
PHOTO 55632

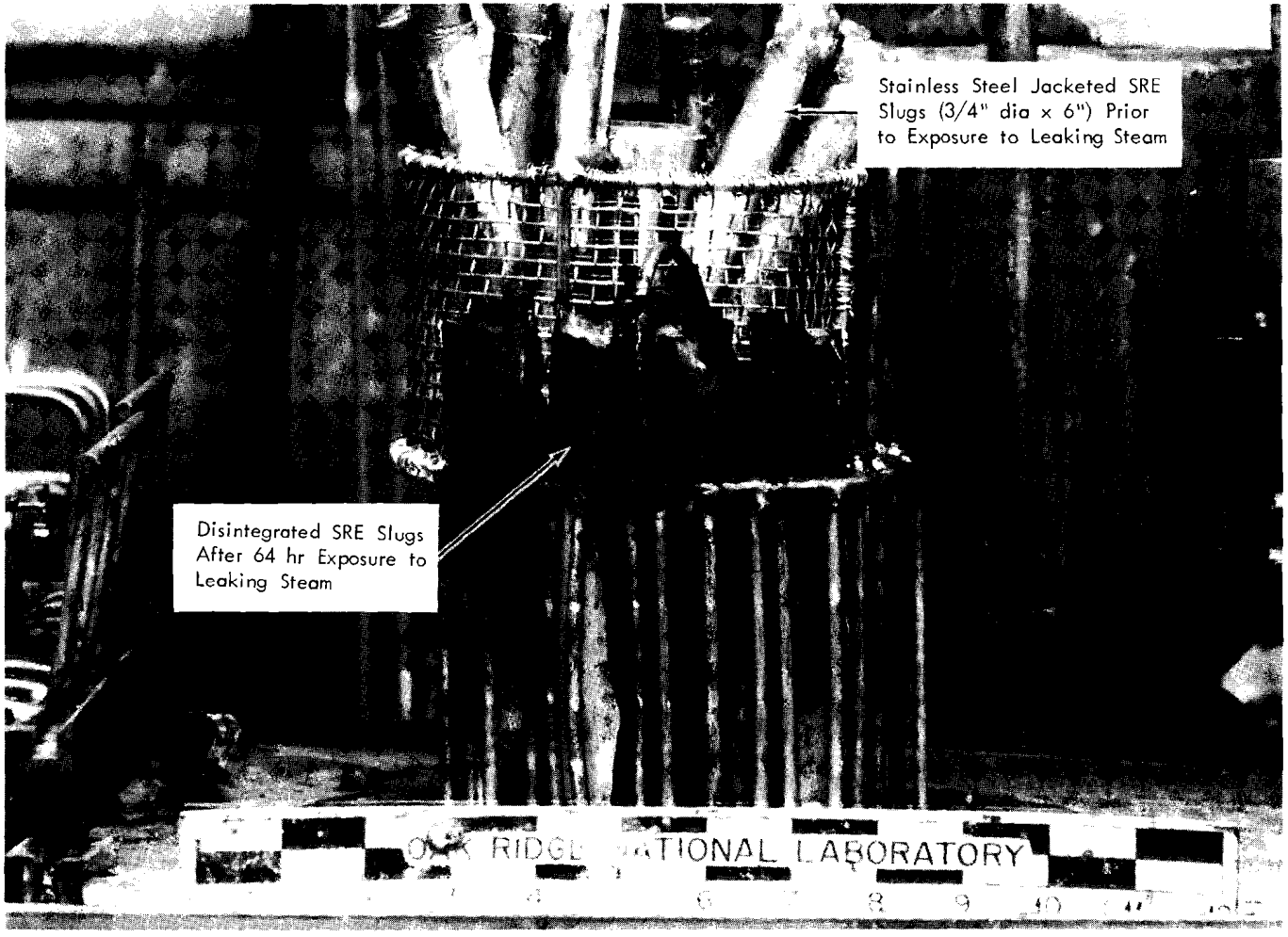

Fig. 3.4. Effect of leaking steam on SRE core I uranium slugs (~ 675 Mwd/ton cooled ~ 2 yrs) (photographed through 5 ft. thick zinc bromide window).

anticipated. Several pieces of equipment were noticeably underdesigned, including: the pneumatically operated tube winder, the hydraulic cylinders for clamping and removing tubing from the collet, and the jackscrew drive and collet mechanism. The hydraulically operated saw leaked at a 1-in. IPS swivel connection in the cell and at two control valves outside the cell due to vibration of the lines. Maintenance this month included replacement of three inner boots on the Model 8 manipulators, the hand grip motor on the General Mills manipulator, and the hand of the Lee Manipulator.

During the final cleanup of NaK from the 25th SRE cluster a minor explosion and fire occurred which was readily extinguished with CO_2. The damage caused by the incident was minor. A one liter glass metering vessel was ruptured and manipulator boot of vinyl-nylon laminate was burned. The incident occurred during the process of transferring NaK from the trough of the hydraulic dejacketing unit to a glass metering pot where a visual quantity measurement is made before the NaK is discharged to a NaK disposal vessel. It is assumed that water was drawn from the reactor vessel or its overhead lines into the metering pot where contact with NaK caused the explosion.

Fifty to seventy-five ml of NaK dispersed in 900 ml of Bayol-D oil were estimated to be involved. A Tygon transfer line connecting the dejacketer trough to the metering pot was severed and the contents of the dejacketer, ~10 gal of oil, was siphoned to the floor. The burning hose kindled the siphoning oil which prompted the manual actuation of the CO_2 fire extinguishing system. The cell ventilation system maintained a negative pressure of 1.0-1.5 in. H_2O throughout the discharge of 20 cylinders, 1500 lbs, of CO_2 to the cell and air monitoring instruments and floor smears revealed that no radioactivity escaped from the cell.

A second fire incident occurred while handling high burnup, 9,500 MWD/t, U-Mo powdered fuel samples. A can of ~300 g of U-Mo alloy, included with the SRE shipment from Atomics Internal for Chemical Development Section B studies, ignited when the contents were opened and agitated for inspection. The fire was smothered by replacing the can's lid and no additional flare-ups were noted. This sample was disposed of by burial underground.

3.3 U-C Fuel Processing - B. A. Hannaford

Recovery of uranium and thorium from graphite fuels by a "semi-continuous" method appears to offer advantages over batch processing for fuels amenable to the nitric acid flowsheets: 90% HNO_3 and grind-leach. To define a semicontinuous flowsheet, experimental data are needed on, (1) the U and Th recovery as a function of contact time and flow rate of leach solution and wash water, and (2) permeability of deep beds of disintegrated fuel to acid and water.

Effect of Contact Time and Flow Rate on U Recovery. An earlier experiment (Unit Operations Monthly Progress Report, July 1961) in which 3/8-in. cubes of graphitized 3% U-graphite fuel were leached for 4.6 hr

in 90% HNO_3 at 60°C, had demonstrated an almost acceptable uranium loss of 0.13%. In an attempt to define the lower limit of acid flow rate for an acceptable uranium loss, a new series of experiments were performed in which total acid contact time was set at 6 hrs and flow rates were varied from 0.51 to 2.0 bed volumes per hour. To increase the surface area of the fuel, the graphite was mechanically crushed to -4 mesh prior to leaching.

Results of the runs are summarized in Table 3.1. Uranium loss in every run was greater than the loss sustained in the earlier experiment with 3/8-in. fuel cubes, despite the longer acid contact time (6 hr vs 4.6 hr), and the higher acid flow rates in runs 105, 106, and 107. The fuel was disintegrated to the same degree in all runs of the current series. Figure 3.5, a plot of uranium inventory in the dissolver vs the flow time, shows that by the end of 120 min acid flow the rate of uranium recovery was diminishing slowly with time. The crossover of runs 106 and 107 at ~80 min may be due to increased channeling which was visually observed at the higher flow rate.

Since the higher uranium losses for runs 104 through 107 (compared to run 101) cannot be attributed to the increase in acid contact time and acid flow rate, they apparently must result from the increased subdivision of the U-graphite fuel charged to the dissolver. Further experiments will be required in order to establish the relationship between feed size and uranium loss.

Table 3.1. Semicontinuous Leaching of -4 Mesh U-Graphite Fuel in 90% HNO_3

Nominal composition of fuel: 3% uranium.
Duration of batch leach period: 2 hr;
Duration of acid flow period: 4 hr;
Duration of water flow period: to clear effluent.
Temperature - 60°C.
Diameter of column: 5 cm

Run No.	Weight of Fuel, g	Height of Bed (final), cm	Mean Particle Size: As Crushed μ	Mean Particle Size: Dried Residue μ	Flow Rate of HNO_3 and H_2O: ml/min	Flow Rate of HNO_3 and H_2O: bed volume/hr	U Loss: ppm in residue	U Loss: %
104	310	21.5	660	330	2.5	0.51	395	1.5
105	323	23.5	660	340	4.5	0.81	417	1.6
106	322	21.6	550	310	7.5	1.5	171	0.61
107	324	23.3	520	270	10.7	2.0	157	0.59

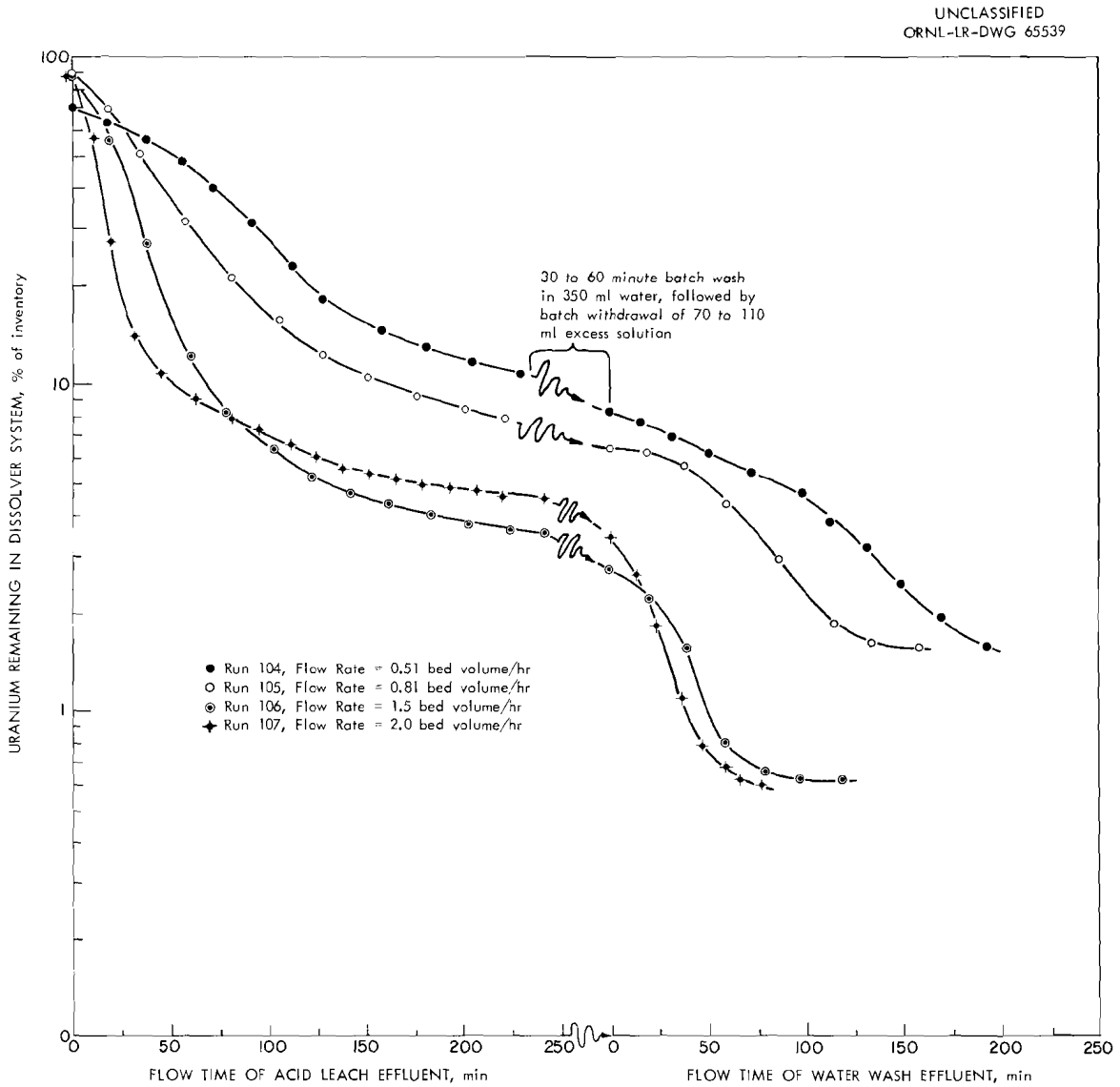

Fig. 3.5. Uranium remaining in dissolver system vs flow time of acid leach and water wash. Final content of graphite residue determined by direct analysis.

4.0 REACTOR EVALUATION STUDIES

J. C. Suddath

4.1 Heat Transfer from Spent Reactor Fuels during Shipping - J. S. Watson

Recently interest has developed in the possibility of aiding heat transfer from spent reactor fuels to the inside walls of shipping casks by packing this space with a solid granular material having a relatively high thermal conductivity. Introduction of the solid material will eliminate any radiation or convection which may have taken place in these spaces, but the effective thermal conductivity of the space may be raised to a value 10 to 20 times that of air. Such a system would be very desirable in casks having very small void spaces and a large portion of the heat transfer is by conduction. In casks where the clearance between the fuel and the wall is relatively large and convection and/or radiation control the heat transfer process, one is likely to find that adding the granular material will actually hinder heat transfer. The usefulness of this technique will also depend upon the ease with which the material may be added and removed from the cask, such as by pouring. However, if the material poures too easily, it is likely to be lost from the cask in an accident. In this case it may be little better than a liquid coolant. However, in some cases it may be possible to advantageously use granular solid coolants.

As noted earlier, the effect of granular coolants on the heat transfer properties of a cask depends upon several parameters of that particular cask (average or effective clearance between the fuel and the cask wall, emissivities of the surfaces, etc.). At least in principal, it is possible to calculate the temperature distribution expected within a cask where all heat transfer is by conduction. Therefore, at least as an initial experimental effort, an attempt was made to evaluate the effective conductivity of a packed bed of a possible suitable coolant, and check certain correlations which have appeared in the literature.[1-5]

A promising type of packing material which can be readily obtained at reasonable cost is the metal shots. A 0.025 in. nominal dia steel shot was obtained from Wheelabrator Corp. for testing. Examination of the material with a microscope showed a relatively high fraction (~20%) of nonspherical particles but an average diameter of approximately 0.019 in. The particles packed to give a porosity (water filled) of 0.404. The density of the individual particles was found to be approximately 7.5 g/cm^3 indicating that they have a very low internal porosity.

For measuring the thermal conductivity of this packing, the material was placed into the annular space between a 5/16-in. heated tube and a 3-in. Sch 40 pipe. The temperatures of the inside surface of the pipe and the surface of the 5/16-in. tube were measured. The tube was identical to those used in previous experiments with simulated fuel bundles (Unit Operations Monthly Report, March 1961) except a thermocouple was welded to the outside surface of the tube. The former experiments had required very low heat fluxes (heat generation rates) and a simple sheathed

thermocouple inserted between the internal heater and tube wall had been adequate. However, in the conductivity experiments the resistance to heat transfer between the tube and pipe walls was much less than in the simulated bundle experiments.

The results of some of the runs are shown in Table 4.1. Along with the experimental temperature and heat generation rates are values of the average thermal conductivity of the bed obtained from the relation

$$\bar{k} = \frac{Q \text{ hr } r_o/r_i}{2\pi(t_i - t_o)}$$

where

$\bar{k}$ = effective conductivity

Q = heat generation rate

r = radii

t = temperature

o,i = subscripts referring to outside and inside of the annular space

Although there are some data scatter, $\bar{k}$ appeared to increase with temperature. This can be expected with granular materials. One can show that if k varies linearly with temperature, $\bar{k}$ will be the k which corresponds to the average temperature, $(t_i + t_o)/2$. Figure 4.1 is a plot of $\bar{k}$ vs $\bar{t}$ and can also be considered a plot of k vs t if k is a linear function of t. Within the scatter of the data they can be fit to a straight line as shown. The results agree reasonably well with literature[1] which predict that the effective conductivity should be approximately 21 times the conductivity of air.

4.2 Estimation of Errors in Temperature Measurements in Simulated Fuel Bundles

The location of thermocouples in simulated fuel bundles without aiding or hindering heat flow presented a problem because of the tight spacings involved. It appeared necessary to bring all leads out of the bundle through the inside of the tubes, and furthermore any exterior protrusions resulting from welding the junction to the tube wall had to be avoided. In view of these restrictions, the arrangement described in the March Unit Operations Monthly Report (ORNL CF 61-3-67) was adopted. A sheathed thermocouple was simply inserted into the tube between the heater and the wall. In principal, this method of measuring the tube wall temperature is poor, and it will always give high readings. However, in this case the method appeared acceptable since the heat fluxes (or heat generation rates) are very low (e.g., the resistance to heat transfer between the tube bundle and the cask wall was very high). If the error in the readings were acceptably low, this method had the advantage of being reasonably simple and temperatures could easily be read at various positions along the length of the tube.

Table 4.1. The Thermal Conductivity of a Bed of Steel Shot

Heat Generation Rate, watts/cm	t_i, °C	t_o, °C	k	
			Cal / sec-cm-°C	Btu / hr-ft-°F
0.799	105	52	0.00136	0.326
0.536	84	46	0.00127	0.306
0.372	67	40	0.00120	0.288
0.196	44.5	30	0.00117	0.282
0.94	118	55	0.00130	0.313
1.05	128	60	0.00134	0.324
1.20	138	63	0.00139	0.338
0.086	35	28.5	0.00117	0.277

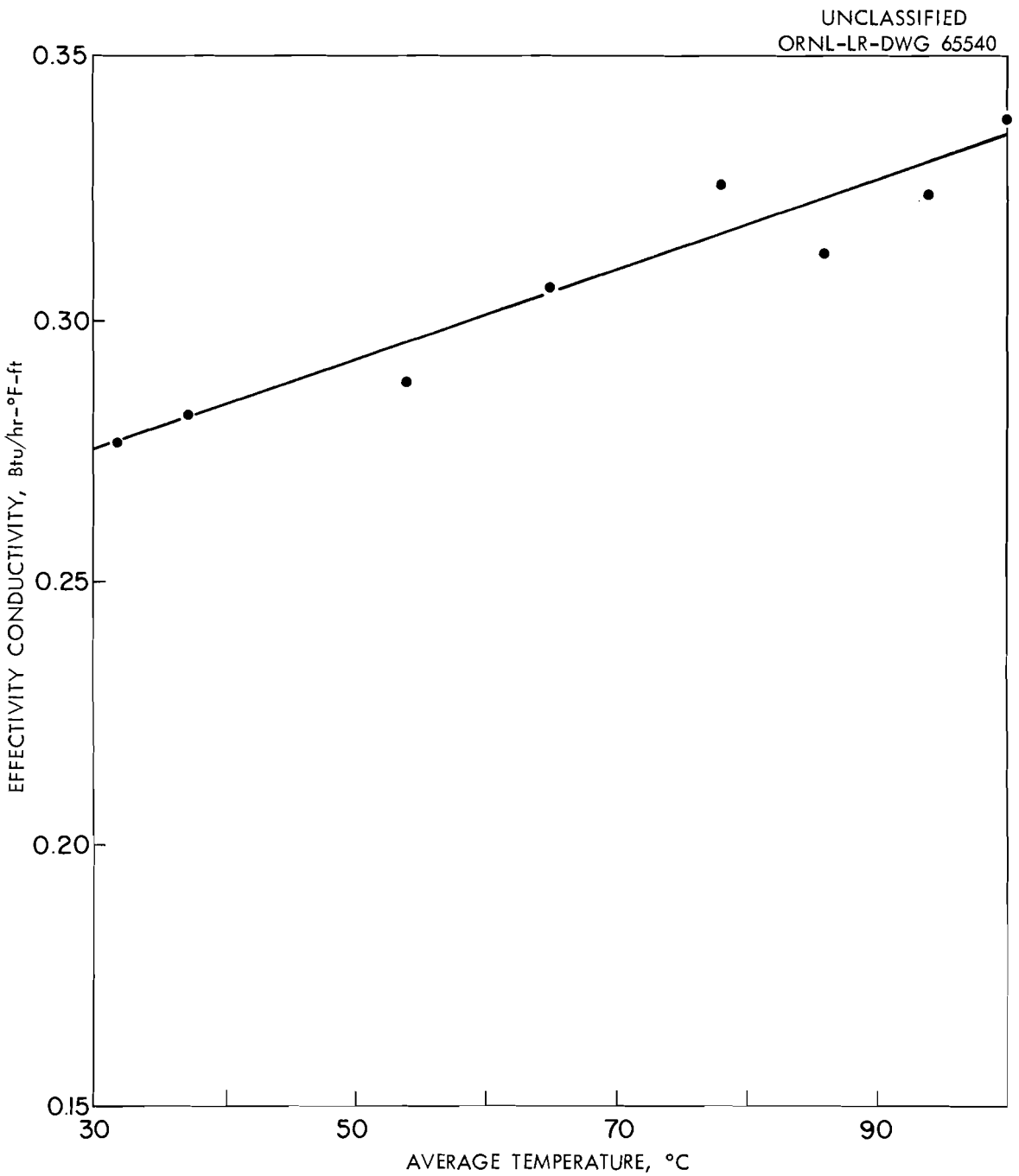

Fig. 4.1. The effect of temperature on the thermal conductivity of a bed of steel shot.

The exact errors to be expected were difficult to calculate because of the relatively complicated geometry of the tube interior, but an error of 3°C was considered acceptable since errors of this magnitude could be expected to result from dimensional uncertainties in assembling the bundles. However, with the thermocouple welded to the side of the tube used in the bed conductivity experiments, a check on the probable temperature errors became possible since the temperature of a sheathed thermocouple inside the tube could also be measured. The difference between the two temperature readings are shown in Figure 4.2 as a function of heat generation rate. Because the thermocouple is not bound rigidly within the tube, some extra scatter is introduced to the data which becomes more evident at higher fluxes. Another factor reducing the linearity of the plot is the increasing conductivity of air within the tube at higher temperatures (which result from higher heat generation rates). Note that in the region used with the simulated fuel bundles, 0.05 watts/cm or less, the error is probably 2°C or less. However, with the higher heat fluxes required for measuring the conductivity of packed steel shot, the error is very significant.

References

1. Deissler, R. G., and J. S. Boegli, "An Investigation of Effective Thermal Conductivities of Powders in Various Gases," Transactions of the ASME, Oct. 1958, p. 1417.

2. Deissler, R. G., and C. S. Eian, "Investigation of Effective Thermal Conductivity of Powders," NACA-RM-E52C05.

3. Godbee, H. W., and J. T. Roberts, "Survey of the Measurements of Thermal Conductivity of Solids Produced by Evaporation and Calcination of Synthetic Fuel Reprocessing Solutions," ORNL-2769.

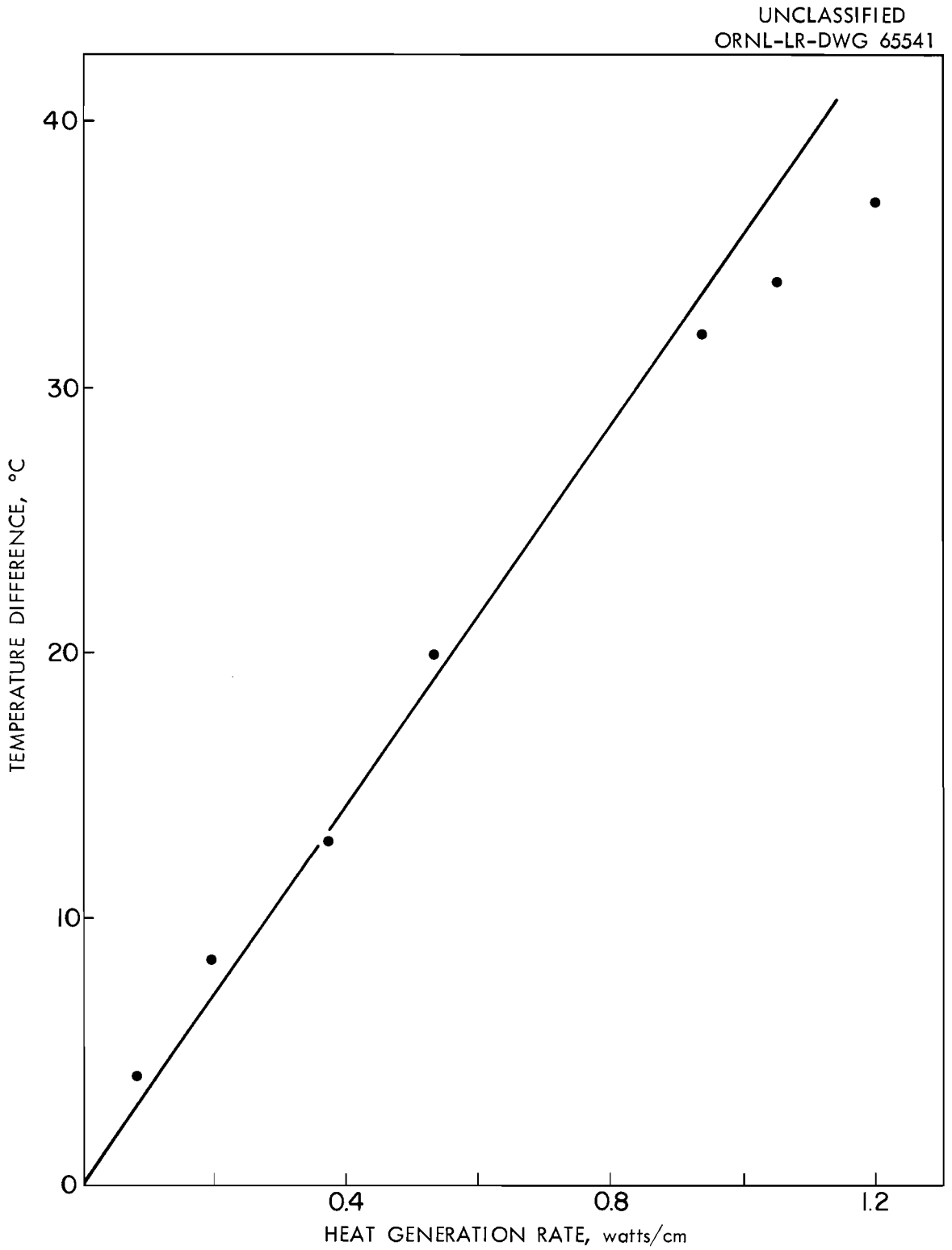

Fig. 4.2. Difference between temperatures measured inside and on the surface of simulated fuel tube.

5.0 SOLVENT EXTRACTION STUDIES

A. D. Ryon

Flooding values reported this month were obtained using the amine extraction flowsheet for final cycle plutonium recovery. The experimental techniques and a description of the pulse columns may be found in the October 1959 Unit Operations Monthly Progress Report (CF 59-10-77).

5.1 Pulse Column Performance Studies - R. S. Lowrie

Work was started this month to evaluate the flow capacity and stage efficiency of a pulse column as a function of operating variables and cartridge design using the amine extraction flowsheet for final cycle plutonium recovery developed by Chemical Development Section C.* Feed for the flowsheet would be the purex partition cycle plutonium product stream containing 1-2 M HNO_3, 0.05 M sulfate and a varying plutonium concentration. A typical flowsheet for the engineering tests (Figure 5.1) used 1.5 M nitric acid containing 0.05 M SO_4 as feed, 0.3 M tertiary amine as solvent, either 0.5 or 5.0 M nitric acid as scrub and 2.0 M acetic acid as stripping reagent. 1.0 M sodium carbonate solution was used as the reagent to the solvent treatment column before recycling the solvent. Lack of containment precluded testing the flowsheet with plutonium present in the feed.

The amine used for this experiment was trilauryl amine, Alamine 304, purchased from General Mills, Inc., Chemical Division, Kankakee, Illinois. It contained < 1% primary, ~7.0% secondary and 93% tertiary amine with a neutral equivalent of 543 and a density of 0.812 g/cc at 25°C. The solvent was made up to be 0.3 M in amine concentration using diethylbenzene as diluent. The diethylbenzene was purchased from Dow Chemical Co., Midland, Michigan, and had a density of 0.861 g/cc, and a viscosity of 0.86 cp at 25°C.

The properties of the test solutions are shown in Table 5.1.

5.2 Flooding Rates for Extraction and Stripping Column

The flooding rates measured in the extraction and stripping columns are shown in Table 5.2. The sieve plate extraction column flooded at 1850 gal $ft^{-2}hr^{-1}$ at 70 cpm using 0.5 M HNO_3 scrub and at a lower flow rate of 1610 gal $ft^{-2}hr^{-1}$ with 5.0 M HNO_3 scrub. Flow capacity was quite high and exceeded the pumping capacity of the equipment at lower pulse frequencies. Flow capacity of the nozzle plate extraction column at 70 cpm was 700 gal $ft^{-2}hr^{-1}$ with 0.5 M nitric scrub and 650 gal $ft^{-2}hr^{-1}$ with 5.0 M nitric scrub. Flooding occurred at 540 gal $ft^{-2}hr^{-1}$ at 35 cpm in the 12 ft sieve plate stripping column using loaded solvent scrubbed with 0.5 M nitric acid and at 440 gal $ft^{-2}hr^{-1}$ at 35 cpm in the 12 ft nozzle plate stripping

---

* K. B. Brown, Chemical Development Section C Progress Report for February-March 1961, p. 27 (CF 61-3-141).

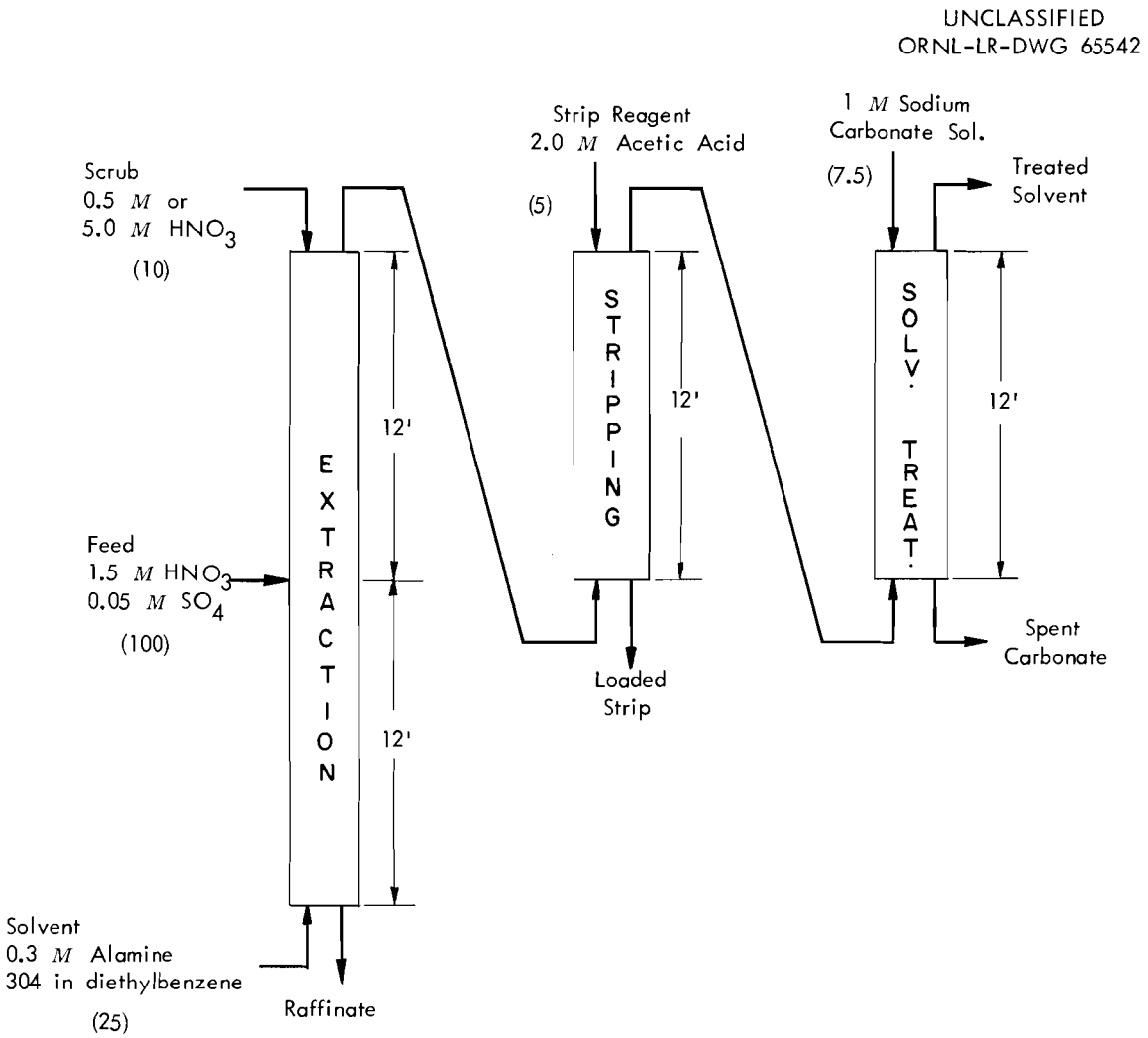

Fig. 5.1. Amine extraction flowsheet for final cycle plutonium recovery.

Table 5.1. Properties of Test Solutions

Analyses	Feed	Scrub A	Scrub B	Strip	Carbonate	Solvent
HNO_3, M	1.5	0.5	5.0	-	-	-
SO_4, M	0.05	-	-	-	-	-
Acetic Acid, M	-	-	-	2.0	-	-
Na_2CO_3, M	-	-	-	-	1.0	-
Density, g/cc	1.05	1.02	1.17	1.01	1.09	0.85
Viscosity, cps	0.90	0.88	1.12	1.05	1.37	1.29
Amine, M	-	-	-	-	-	0.32
Flash Point	-	-	-	-	-	-
Open Cup, °C	-	-	-	-	-	64

Density and viscosity measured at 25°C.

Table 5.2. Flooding Rates for Extraction and Stripping Columns

Column	Phase Continuous	Pulse Frequency cpm	Flooding Rate-gal $ft^{-2}hr^{-1}$ 0.5 M HNO_3 Scrub	5.0 M HNO_3 Scrub
Extraction Column				
Sieve plate	Aq	50	> 2400	-
		70	1850	1610
		90	1160	-
Nozzle plate	Solv	30	1590	1460
		50	920	870
		70	700	650
		90	< 300	-
Stripping Columns				
Sieve plate	Aq	25	540	650
		35	540	560
		50	300	400
		70	130	-
Nozzle plate	Solv	35	440	484
		50	290	-

Pulse amplitude = 1 inch.
Sieve plates contained 0.125-in.-dia holes, 23% free area.
Nozzle plates contained 0.125-in.-dia nozzles, 10% free area.

column using the same solvent. Flow capacity for both columns increased slightly with loaded solvent scrubbed with 5.0 M nitric acid. Sieve plate columns were operated with the aqueous phase continuous, nozzle plate columns with the organic phase continuous.

5.3 Flooding Rates of Solvent Treatment Columns

In general, alkaline wash treatments are required to clean up the stripped solvent before recycle. Neither the amount of solvent cleanup nor the reagent to be used have been adequately defined. Flooding tests were made using 1 M sodium carbonate solution by arbitrary choice. Solvent coming from the strip column contains the equivalent of 0.6 N acid (as both free acid and amine salt) which reacts with the sodium carbonate to form CO_2. Tests were carried out at aqueous solvent ratios of 1/2 and 1/3.3, equivalent to 60 and 100% utilization of the carbonate. Flooding rates for aqueous continuous operation of the sieve plate columns at a 1/2 phase ratio increased from 270 to 375 gal $ft^{-2}hr^{-1}$ as pulse frequency decreased from 50 to 35 cpm (Table 5.3). The column was inoperable due to excessive gassing at phase ratio of 1/3.3. Conversely, the column could not be flooded with the available flows when operated organic continuous at 1/3.3 phase ratio. Flow capacity of the nozzle plate column operated organic continuous at 1/3.3 phase ratio increased from 290 to 350 gal ft^{-2} hr^{-1} as the pulse frequency decreased from 50 to 35 cpm.

Table 5.3. Flooding Rates of Solvent Treatment Columns

Column	Phase Ratio A/O	Phase Cont.	Pulse Freq. cpm	Flooding Rate gal $ft^{-2}hr^{-1}$
Sieve plate	1/2.0	Aq	35	375
0.125-in.-dia			50	270
holes	1/3.3	Aq	35	< 100
23% free area			50	< 100
	1/3.3	Solv	35	(No flooding at maximum
			70	(flow available >700
			110	
Nozzle plate	1/3.3	Solv	35	350
0.125-in.-dia			50	290
nozzles				
10% free area				

Pulse amplitude = 1 inch.

6.0 WASTE PROCESSING

J. C. Suddath

Development studies on engineering-scale equipment were continued to obtain design information for flowsheet and control analysis. During this period several tests were made using simulated Purex and TBP-25 type waste and operating with the continuous and batch evaporator.

6.1 Evaporator-Calciner Studies - C. W. Hancher

Engineering-scale studies were continued to obtain design data for the high level pilot plant flowsheets. The major effort was on Idaho Chemical Plant type waste (TBP-25), since this is the proposed first feed for the pilot plant. Tests were made in the large batch evaporator-calciner system and in the small continuous evaporator-calciner system. A summary of test conditions and results is presented in Table 6.1. Tests R-42 and R-43 have been analyzed in detail in Tables 6.2 and 6.3. The remaining tests will be analyzed and will appear in a later Unit Operations Monthly Reports.

Average feed rates decreased with prolonged feed periods, but the bulk density of the calcined solids increased for the long feed periods. An economic stopping point may be determined by balancing operating time against basic fixed cost. In report ORNL-TM-59, J. J. Perona calculated that a pot 12-in.-dia should be approximately 99.1% full for economic optimum filling.

Stable ruthenium was added to the feed for five of the tests to determine the volatility under evaporator operating conditions. The ruthenium in the condensate was below analytical detection except during minor upsets at the start of each test.

Control of both the batch and continuous systems was good, except for feed line plugging at high concentrations which would upset control of the entire system. The boil-up rate of the continuous evaporator was insufficient at the peak rate for the Purex flowsheet, but has been corrected by removing a mitered 90° elbow (2 in. IPS) on the discharge of heat-exchange and replacing it with a smooth radial sweep elbow (3 in. IPS) that returns the discharge of steam chest above the evaporator level instead of below as former line did. The boil-up rate was increased from 6-8 liters per min to greater than 12 liter/min.

Table 6.1. Summary of Conditions and Results

Test No.	Feed Type	System	Calciner Feed Concentration Factor	Water to Feed Ratio for Test liter/liter	Off-gas to Feed Ratio for Test ft^3/liter	Nitrate in Calcined Solids Wt %	Bulk Density of Calcined Solids g/cm^3	System Feed Rate Average for Feed Period liter/hr
42	Purex	Continuous	1.18 to 1.96	4.4	~	0.02 - 2.3	1.5	49
43	Purex	Continuous	1.3 to 2.2	Leak	1.09	0.008 - 0.9	1.28	50.0
44	Purex	Continuous	1.3 to 3.8	7.8	2.02	0.06 - 0.14	1.14	40.9
45	Purex	Batch	0.98 to 1.35	3.9	2.20	0.01 - 4.7	1.17	25.2
46	Purex	Batch	0.98 to 1.27	4.1	3.50	0.01 - 3.7	1.55	25.8
47	TBP-25	Continuous	1.2 to 2.3	3.4	1.90	0.36 - 6.0	0.57	30.6
48	TBP-25	Continuous	0.93 to 1.6	2.8	3.50	0.10 - 6.0	0.77	15.0

Table 6.2. Results and Conditions for Test R-42

Feed Concentrations

	H^+ M	HNO_3 M	Fe g/ℓ	Na g/ℓ	$SO_4^=$ g/ℓ	Ru g/ℓ
As madeup	5.1	6.1	25.0	13.0	96.0	0.15
As analyzed						
Tank 1	5.57	6.27	28.8	13.3	97.5	0.160
Tank 2	5.44	6.32	28.9	12.1	93.8	0.166
Tank 3	5.00	5.84	30.6	13.3	102.0	0.183

System Balances and Results

NO_3 Balance		
Input:	3735 g moles	
Recovery:		
Condensate	4006 g moles	107.2%
Solid	107 g moles	2.8%
Evap.	47.5 g moles	1.3%
Off-gas	-	-
		111.3%
Fe Balance		
Input:	263 g moles	
Recovery:		
Condensate	1.6 g moles	0.6%
Solid	229 g moles	87.1%
Evap.	10.1 g moles	3.8%
		91.5%
Na Balance		
Input:	287 g moles	
Recovery:		
Condensate	1.5 g moles	0.8%
Solid	245 g moles	88.1%
Evap.	5.4 g moles	1.9%
		90.8%
SO_4 Balance		
Input:	505 g moles	
Recovery:		
Condensate	5.8 g moles	1.2%
Solid	466 g moles	92.3%
Evap.	19.2 g moles	3.8%
		97.3%

Table 6.2. Continued

Ru Balance

Input:	0.827 g moles	
Recovery:		
Condensate	-	-
Solid	0.379 g moles	45.8%
Evap.	0.049 g moles	5.9%
		51.7%

Average Feed Rate

495.5/10 = 49.55 liters/hr average

Water Feed Rate

2195 liters of water, water to feed ratio = 4.4

Calcined Solids

90 kg solids/60 liters = 1.50 g/cc bulk density

Solid Analysis

	Fe wt %	Ru wt %	Ca wt %	Al wt %	NO_3 wt %	SO_4 wt %	Na wt %
S-1	10.8	0.044	15.7	1.10	2.37	54.06	5.68
S-2	10.1	0.062	23.6	0.91	0.63	40.70	5.04
S-3	16.7	0.045	11.2	1.10	0.03	52.39	7.44
S-4	19.3	0.022	9.5	1.02	0.02	51.50	6.88
Average	14.2	0.043	10.5	1.03	0.76	49.66	6.26

Table 6.3. Results and Conditions for Test R-43

Feed Concentrations

	H^+ M	HNO_3 M	Fe g/ℓ	Na g/ℓ	SO_4 g/ℓ	Ru g/ℓ
As madeup	5.1	6.1	25.0	13.0	96.0	0.15
As analyzed						
Tank 1	5.10	5.84	26.1	12.6	92.3	0.126
Tank 2	5.20	6.22	27.2	13.4	93.9	0.157
Average	5.15	6.03	26.6	13.0	93.1	0.141

System Balances and Results

NO_3 Balance		
Input:	3582 g moles	
Recovery:		
Condensate	2927 g moles	81.7%
Solid	0.2 g moles	-
Evap.	1.9 g moles	0.1%
		81.8%
Fe Balance		
Input:	268 g moles	
Recovery:		
Condensate	2.3 g moles	0.9%
Solid	178.3 g moles	66.5%
Evap.	0.02 g moles	-
		67.4%
Na Balance		
Input:	336 g moles	
Recovery:		
Condensate	2.3 g moles	0.7%
Solid	109 g moles	32.5%
Evap.	0.06 g moles	-
		33.2%
SO_4 Balance		
Input:	576 g moles	
Recovery:		
Condensate	5.8 g moles	1.0%
Solid	453 g moles	78.7%
Evap.	0.09 g moles	-
		79.7%

Table 6.3. Continued

Ru Balance

Input:	0.820 g moles	
Recovery:		
Condensate	-	-
Solid	0.32 g moles	39.7%
Evap.	-	-
		39.7%

Off-Gas

649/594 = 1.09 cu ft/liter of system feed

Average Feed Rate

594/8 = 74.2 liter/hr average

Water Feed Rate

3698 liters of water

Calcined Solids

76.4 kg solid/60 liters = 1.28 g/cc bulk density

Solid Analysis

	Fe wt %	Ca wt %	SO_4 wt %	Na wt %	NO_3 wt %	Ru ppm
Top 1	9.26	0.03	58.9	2.95	0.90	353
2	18.40	0.02	58.2	4.49	0.008	502
3	9.06	0.04	53.5	1.30	0.18	353
Bottom 4	16.10	0.02	59.0	4.04	0.014	434
Average	13.3	0.028	57.3	3.2	0.30	432

DISTRIBUTION

1. E. L. Anderson (AEC Washington)
2. F. P. Baranowski (AEC Washington)
3. W. G. Belter (AEC Washington)
4. S. Bernstein (Paducah)
5. R. E. Blanco
6. J. O. Blomeke
7-10. J. C. Bresee
11. R. E. Brooksbank
12. K. B. Brown
13. F. R. Bruce
14. J. A. Buckham (ICPP)
15. L. P. Bupp(HAPO)
16. W. D. Burch
17. W. H. Carr
18. G. I. Cathers
19. J. T. Christy (HOO)
20. W. E. Clark
21. V. R. Cooper(HAPO)
22. K. E. Cowser
23. F. E. Croxton (Goodyear Atomic)
24. F. L. Culler, Jr.
25. W. Davis, Jr.
26. O. C. Dean
27. D. E. Ferguson
28. L. M. Ferris
29. R. J. Flanary
30. E. R. Gilliland (MIT)
31. H. E. Goeller
32. M. J. Googin (Y-12)
33. H. B. Graham
34. A. T. Gresky
35. P. A. Haas
36. M. J. Harmon (HAPO)
37. F. E. Harrington
38. L. P. Hatch (BNL)
39. O. F. Hill (HAPO)
40. J. M. Holmes
41. R. W. Horton
42. A. R. Irvine
43. G. Jasny (Y-12)
44. H. F. Johnson
45. W. H. Jordan
46. S. H. Jury
47. K. K. Kennedy (IDO)
48. B. B. Klima
49. E. Lamb
50. D. M. Lang
51. S. Lawroski (ANL)
52. R. E. Leuze
53. W. H. Lewis
54. J. A. Lieberman (AEC Washington)
55. R. B. Lindauer
56. A. P. Litman
57. J. T. Long
58. B. Manowitz (BNL)
59. J. L. Matherne
60. J. A. McBride (ICPP)
61. J. P. McBride
62. W. T. McDuffee
63. R. A. McGuire (ICPP)
64. R. P. Milford
65. J. W. Morris (SRP)
66. E. L. Nicholson
67. J. R. Parrott
68. F. S. Patton, Jr. (Y-12)
69. H. Pearlman (AI)
70. R. H. Rainey
71. J. T. Roberts (IAEA, Vienna, Aust.)
72. K. L. Rohde (ICPP)
73. C. A. Rohrmann (HAPO)
74. A. D. Ryon
75. W. F. Schaffer, Jr.
76-78. E. M. Shank
79. M. J. Skinner
80. C. M. Slansky (ICPP)
81. S. H. Smiley (ORGDP)
82. J. I. Stevens (ICPP)
83. C. E. Stevenson (ANL, Idaho)
84. K. G. Steyer (General Atomics)
85. E. G. Struxness
86. J. C. Suddath
87. J. A. Swartout
88. F. M. Tench (Y-12)
89. V. R. Thayer (duPont, Wilmington)
90. W. E. Unger
91. J. Vanderryn (AEC ORO)
92. F. M. Warzel (ICPP)
93. C. D. Watson
94-123. M. E. Whatley
124. G. C. Williams
125. R. H. Winget
126. R. G. Wymer
127-128. Central Research Library
129-132. Laboratory Records
133. Laboratory Records (RC)
134. Document Reference Section
135. Research and Development Division
136-150. DTIE